Research Square

Preprints are preliminary reports that have not undergone peer review.
They should not be considered conclusive, used to inform clinical practice,
or referenced by the media as validated information.

Exploratory Feasibility Study: Vibration-Induced Kinesthetic Illusion Intensity Correlates with Motor Planning and Control Brain Activation

Filip Španiel
filip.spaniel@nudz.cz

National Institute of Mental Health
David Tomeček
National Institute of Mental Health
Jan Kubr
VR medical s.r.o.
Eduard Bakštein
National Institute of Mental Health
Karolína Zuzánková
National Institute of Mental Health
Konstantin Novikov
VR medical s.r.o.
Robert Zajíček
University Hospital Kralovske Vinohrady
Bohumil Bakalář
University Hospital Kralovske Vinohrady
Tereza Dědičová
VR medical s.r.o.
Vlastimil Koudelka
National Institute of Mental Health
Iveta Fajnerová
National Institute of Mental Health

Short Report

Keywords: Kinesthetic Illusion, fMRI, Vibration Stimulation, Brain Activation

Posted Date: September 29th, 2026

DOI: https://doi.org/10.21203/rs.3.rs-11000729/v1

License: This work is licensed under a Creative Commons Attribution 4.0 International License. Read Full License

Additional Declarations: Competing interest reported. Authors Jan Kubr, Konstantin Novikov, and Tereza Dědičová are employees of VRmedical, the developer of the technical solution described in this manuscript. The authors declare no other competing interests.

Abstract

Objectives: Kinesthetic illusions (KI), defined as the perception of movement without actual limb motion, can be induced via tendon vibration and engage motor-related brain regions. This pilot fMRI study examined the relationship between KI vividness and neural activation.

Methods: Five healthy right-handed participants (mean age 27 ± 5.4 years) underwent fMRI during pneumomechanically induced vibration at the dominant wrist to elicit KI. An activation paradigm with four runs, each using varying stimulation parameters, was applied. After each run, participants rated KI vividness on a 0–4 scale. Neural activation was analyzed, and associations with subjective ratings were assessed using a linear mixed-effects model.

Results: Significant activation ($p < 0.001$, uncorrected) was observed in regions associated with action selection, motor initiation, and internal movement simulation. KI vividness ratings were positively correlated with ROI activation ($\beta = 2.62$, standard error = 0.73, $p = 0.012$, $R^2 = 0.44$).

Conclusions: Greater KI vividness is associated with increased activation in motor-related brain regions, suggesting that KI may enhance neural engagement. These findings support the potential of KI as a non-invasive approach to stimulate motor circuits and promote neuroplasticity. Due to the small sample size, results should be considered preliminary and hypothesis-generating.

Introduction

The kinesthetic illusion (KI) is the perception of limb movement or displacement in the absence of actual movement. It arises when sensory inputs related to proprioception or muscle activity are manipulated, causing the brain to interpret movement that does not occur. KI can be vividly induced by high-frequency vibration (80-100 Hz) applied to a muscle tendon, which activates muscle spindle afferents and mimics the sensory signals of actual muscle stretch, creating a strong illusion of joint movement without physical motion [1,2].

Neuroimaging studies consistently show that vibration-induced KI engages motor-related regions. PET studies identified activation of the primary motor and premotor cortices, supplementary motor area (SMA), and insula [3–6], while subsequent fMRI studies confirmed involvement of a broader sensorimotor network, including sensorimotor cortex (S1/M1), SMA cerebellum, inferior parietal lobule, and premotor cortex [7–10]. EEG studies further characterized the temporal dynamics of this network through event-related desynchronization patterns, supporting an overlap between KI, motor imagery, and movement execution [11, 12]. Posterior parietal involvement has also been demonstrated during the integration of conflicting visual and kinesthetic information [8, 13, 14]. Together, these findings indicate that KI recruits neural networks involved in sensorimotor processing and internal movement representation.

By activating motor-related brain regions without actual movement, KI has potential as a neurorehabilitation approach, potentially supporting neuroplasticity through congruent sensory input [15], while engaging restorative and compensatory pathways. Accordingly, KI may support recovery in individuals affected by stroke, burns, or other forms of prolonged immobility. Its effects may depend on illusion vividness, yet it remains unclear whether stronger subjective KI is associated with greater neural engagement. Therefore, this exploratory pilot fMRI study examined the association between KI vividness and activation in motor-related brain regions during wrist tendon vibration in healthy participants. We hypothesized that greater KI vividness would be associated with stronger motor-related activation.

Methods

1.1 Participants

Five healthy, right-handed volunteers (mean age: 27.0 ± 5.39 years; gender: three female, two male) participated in this pilot study after providing written informed consent.

1.2 Experimental Procedure

During scanning, participants lay supine with their right arm positioned alongside the body and the wrist secured in foam padding to minimize motion. Participants remained at rest. Four runs were performed for each participant, each involving tendon vibration with different stimulation parameters, as described below. After each run, participants verbally rated the vividness of the kinesthetic illusion on a 5-point scale from 0 to 4, where 0 indicated no illusion of movement, and 4 indicated the most vivid illusion.

1.3 Pneumatic Vibration Device

A pneumomechanical actuator was constructed entirely from MRI-compatible, 3D-printed polymers so that no ferromagnetic or conductive components entered the scanner bore. Its core is an air-driven “excenter” (eccentric rotor) housed in a sealed chamber; two interchangeable rotors (masses 2.3 g and 4.7 g) generate different vibration frequencies. Compressed air from a remote compressor (located outside the magnet room) is delivered through a 10 m silicone hose to a two-position regulator, which switches between 3 bar and 4 bar. The rotor spins against an extended exhaust channel (to prevent local heating or uncomfortable airflow on the participant’s wrist). An adjustable strap secures the chamber flush against the volar wrist, ensuring stable contact with the underlying flexor tendons.

Rotor mass and inlet pressure were calibrated against output frequency prior to experiments. At 4 bar, the lighter (2.3 g) rotor produced approximately 100 Hz, whereas the heavier (4.7 g) rotor produced approximately 80 Hz. Reducing the inlet pressure to 3 bar lowered each frequency by roughly 20 Hz: the 2.3 g rotor yielded ~80 Hz, and the 4.7 g rotor yielded ~60 Hz. This two-by-two configuration (low vs. high mass, 3 bar vs. 4 bar) provided four distinct stimulation

conditions characterized by specific combinations of frequency and amplitude. The manipulation of both rotor mass and air pressure ensured that these conditions provided a range of vibration intensities; due to the physics of eccentric mass vibration, increasing the rotor mass at a given frequency increases the resultant centrifugal force and vibration amplitude. Thus, the design allowed us to explore different levels of proprioceptive stimulation beyond simple frequency modulation, while providing repeatable vibration frequencies, with no electronic components near the scanner. Accelerometer data (Brüel & Kjær Type 4525B) in free and wrist-mounted setups confirmed peak frequencies around 100 Hz (also measured at 92, 96, 104, 108, 112 Hz), showing consistent generation of the target oscillations. Pilot fMRI scans with the actuator strapped to the volar wrist—both idle and active—showed no additional motion artifacts compared to baseline imaging.

1.4 Experimental Paradigm

To induce a range of kinesthetic illusion intensities for the correlation analysis, we employed a 2 × 2 factorial design manipulating rotor mass (lighter vs. heavier excenter) and air pressure (3 bar vs. 4 bar). Four separate runs—one for each combination of mass and pressure—were conducted in random order for each participant. Each four-minute run consisted of six cycles of 20 s vibration alternating with 20 s rest. The participant remained motionless and verbally reported comfort and perceived KI intensity after each run. The time interval between the four consecutive runs was 1.9 minutes on average.

1.5 Data Acquisition

MRI data were acquired using a 3 Tesla Siemens Prisma scanner with a standard 64-channel head coil. High-resolution structural 3D images were collected for anatomical reference using a T1-weighted (T1w) magnetization-prepared rapid gradient echo (MPRAGE) sequence with the following parameters: repetition time (TR) = 2400 ms, echo time (TE) = 2.3 ms, flip angle = 8°, voxel size = 0.7 × 0.7 × 0.7 mm^3, matrix size = 320 × 320, field of view (FOV) = 224 × 224 mm, and 240 sagittal slices. Functional images were acquired using a T2*-weighted (T2*w) gradient echo-planar imaging (GR-EPI) sequence sensitive to the blood oxygenation level-dependent (BOLD) signal, with the following parameters: TR = 1000 ms, TE = 30 ms, flip angle = 52°, voxel size = 2 × 2 × 2 mm^3, matrix size = 104 × 104, FOV = 208 × 208 mm, 64 axial slices per volume (using a multiband acceleration factor of 4), and 240 volumes in total.

1.6 Data Preprocessing

All structural and functional images were converted from DICOM to NIFTI format using the dcm2niix tool (https://github.com/rordenlab/dcm2niix). Preprocessing was conducted in MATLAB (The MathWorks, Inc., Natick, MA, USA) using the CONN toolbox v21a (https://web.conn-toolbox.org/), employing the default preprocessing pipeline for volume-based analyses.

Preprocessing of functional images included bias field correction, realignment and unwarping, slice-timing correction, segmentation and normalization to MNI space, and spatial smoothing with an 8 mm full-width-at-half-maximum (FWHM) Gaussian kernel. Structural images were segmented and normalized to MNI space.

1.7 Data Analysis

For each subject and session, first-level general linear model (GLM) analyses were conducted to model the effects of a stimulation condition (six 20-second blocks of vibration-induced kinesthetic illusion) and a control condition (six 20-second blocks of resting), including six motion parameters (translations and rotations along all three axes) as nuisance regressors. Contrast maps comparing stimulation to the control condition were computed to estimate the main effect of stimulation. These first-level contrast maps were then entered into a second-level flexible factorial model to account for repeated measurements within each subject, the effects of experimental conditions, and to assess the group-level effect of stimulation. To further investigate whether stimulation effects were connected to individual KI vividness rating for each adapter/pressure combination, a second-level statistical map thresholded at $p < 0.001$ (uncorrected for multiple comparisons) was used to define a region of interest (ROI) with the MarsBaR toolbox (https://marsbar-toolbox.github.io/). Beta weights from each subject's first-level contrast map were extracted within this ROI to differentiate stimulation from baseline, and the median beta coefficient across the ROI was used to represent the activation level.

A linear mixed-effects model with a random intercept for each participant was used to account for repeated measures and potential individual offsets (KI vividness rating ~ Activation + condition + (1|subjectID)) to evaluate the relationship between activation and KI vividness ratings. The experimental condition was included in the linear mixed-effects model as a fixed effect to account for the systematic variance introduced by the different stimulation parameters, although the primary focus was the relationship between subjective vividness and brain activation. Inclusion of random slopes was investigated but led to singular or unstable model fits. The statistical analyses were performed in R using RStudio (https://www.R-project.org/). Mixed-effects models were estimated using the lme4 package [16], and significance was assessed using Satterthwaite's method in the lmerTest package [17].

Results

2.1 Group-Level Results

We observed significant stimulation-related activation at the group level in several brain regions (see Fig. 1; threshold: $T = 3.93$, $p < 0.001$, uncorrected for multiple comparisons). These regions included the right inferior frontal gyrus (opercular part), left inferior frontal gyrus (triangular part), bilateral middle frontal gyrus, bilateral precentral gyrus, the bilateral supplementary motor area, right supramarginal gyrus, left postcentral gyrus, bilateral caudate nucleus,

left thalamus, and bilateral insula. Additionally, the following cerebellar regions and vermis were included: bilateral cerebellar lobe VI, bilateral cerebellar crus II, right cerebellar crus I, vermis lobule IX, bilateral cerebellar lobe VIII, and left cerebellar lobe VIIb. Reported activations were uncorrected; findings should be interpreted with caution due to the increased risk of false positives. For the complete list of activated regions, see Table S1.

2.2 Subjective kinesthetic-illusion ratings and cortical activation magnitude

We fitted a linear mixed model with random intercept to predict KI vividness rating from activation level (median beta within the ROI). The effect of median ROI beta was statistically significant and positive (beta = 2.62 (std. error 0.73), t(5.9) = 3.59, p = 0.012), indicating that higher activation was associated with higher KI vividness ratings - see Fig. 2. The model's explanatory power related to the fixed effects alone (marginal R2) was 0.44.

Discussion

Our study aimed to elucidate the neural correlates of kinesthetic illusions using functional MRI by characterizing the pattern of brain activation during illusion-inducing stimulation. At the group level, significant stimulation-related activation was observed in a distributed network including the right inferior frontal gyrus (opercular part), left inferior frontal gyrus (triangular part), bilateral middle frontal gyrus, bilateral precentral gyrus, bilateral supplementary motor area, right supramarginal gyrus, left postcentral gyrus, bilateral caudate nucleus, left thalamus, bilateral insula, and several cerebellar regions. This pattern is consistent with the engagement of brain systems involved in motor planning, sensorimotor integration, bodily awareness, and movement-related coordination. Activation in the bilateral precentral gyri and supplementary motor area is compatible with internal movement representation in the absence of overt movement, in line with previous work showing recruitment of motor-related regions during kinesthetic illusion and motor imagery [3, 4, 18–20]. The right supramarginal gyrus and left postcentral gyrus suggest involvement of parietal and somatosensory mechanisms relevant to proprioceptive integration and body-state updating [21], while bilateral insular activation may reflect interoceptive and subjective aspects of the illusion experience [22]. In addition, activation in the bilateral caudate nucleus and left thalamus is compatible with the contribution of subcortical circuits implicated in action selection and sensorimotor processing [23–25]. Because these findings were identified at an uncorrected threshold, they should be interpreted cautiously.

Motor-related cortical regions were represented in the observed activation pattern, particularly the bilateral precentral gyri and supplementary motor area. Therefore, the current findings can be interpreted as evidence of a distributed cortico-subcortical-cerebellar network that supports kinesthetic illusion. This interpretation is broadly consistent with previous studies showing that vibration-induced kinesthetic illusion recruits sensorimotor, premotor, parietal, and cerebellar systems associated with internally generated movement experience [3, 4, 6, 8–10].

Our analysis examined the relationship between the intensity of kinesthetic illusion and brain activation. Using a linear mixed model, we found a significant positive correlation between subjective kinesthetic illusion intensity and activation within the stimulation-defined ROI, indicating that more vivid illusions were associated with stronger task-related neural responses.

This finding holds clinical promise, as sustained brain activation promotes neuroplasticity—a key mechanism in neurorehabilitation [26]. While the rehabilitative potential of highly engaging kinesthetic experiences remains empirically unverified, our results support this compelling hypothesis and highlight the need for targeted investigation.

Limitations

This study offers preliminary insights but is constrained by several significant limitations. The small, homogeneous sample (N = 5; young, right-handed, healthy adults) limits generalizability, particularly to clinical populations. The fMRI data were analyzed without multiple-comparisons correction, increasing the likelihood of false positives. Additionally, brain activation data were used to generate the mask and to conduct second-level ROI-based correlations with self-reported vividness. While this raises the possibility of circular inference, using the main effect of stimulation (vibration > rest) to define ROIs preserves statistical independence, as it is orthogonal to the vividness ratings. Illusion intensity was assessed subjectively and only after each run, introducing potential recall bias and reducing temporal accuracy. Implementing real-time or continuous feedback during stimulation would likely improve measurement reliability. Given these limitations, this study serves as a proof of concept intended to guide the design of future research. Subsequent studies should build on these preliminary findings by using larger, more diverse samples, validated stimulation tools, real-time feedback mechanisms, and appropriate statistical corrections. These advancements will be essential for translating early insights into clinically relevant applications.

Abbreviations

BOLD
Blood oxygenation level-dependent
DICOM
Digital Imaging and Communications in Medicine
EEG
Electroencephalography
fMRI
Functional magnetic resonance imaging
FOV
Field of view
FWHM

Full width at half maximum
GLM
General linear model
GR-EPI
Gradient echo-planar imaging
KI
Kinesthetic illusion
M1
Primary motor cortex
MNI
Montreal Neurological Institute
MPRAGE
Magnetization-prepared rapid gradient echo
MRI
Magnetic resonance imaging
NIfTI
Neuroimaging Informatics Technology Initiative
PET
Positron emission tomography
ROI
Region of interest
S1
Primary somatosensory cortex
SMA
Supplementary motor area
TE
Echo time
TR
Repetition time

Declarations

Ethics approval and consent to participate

This study was performed in line with the principles of the Declaration of Helsinki. Approval was granted by the Ethical Committee of the National Institute of Mental Health in Klecany, Czech Republic (No. 152/23). Informed consent for participation and publication was obtained from all individual participants in written form.

Consent for publication

Not applicable. The manuscript does not contain any identifiable individual participant data.

Availability of data and material

The dataset is currently undergoing final processing at Zenodo and should become publicly accessible under these links and doi: https://zenodo.org/uploads/15630957, alias https://doi.org/10.5281/zenodo.15630957

In the meantime, for the purposes of the peer-review process, the dataset can be accessed via the following read-only link:

https://zenodo.org/records/15630957?preview=1&token=eyJhbGciOiJIUzUxMiJ9.eyJpZCI6Ijc2NmE1NmFiLTViNDYtNGMyZS1hMjBmLWIxZmYyZmJlMjNmYSIsImRhdGEiOnt9LCJyYW5kb20iOiJjZDlN2M1MTg5NjU2OThhODFkMjE5YiJ9.hj57e2HjPQdozk0eoZAGhMQ3kkKYqnDBLu_Ev6_GY91c7OMIgLCgwkxvLC5NYM101AXp-qi-iUWBmD6Fg1H0Qw

Competing interests

Authors Jan Kubr, Konstantin Novikov, and Tereza Dědičová are employees of VRmedical, the developer of the technical solution described in this manuscript. The authors declare no other competing interests.

Funding

This work was supported by the Technology Agency of the Czech Republic, program TREND, grant no. FW06010562 titled “A unique combination of virtual reality and kinesthetic illusions in rehabilitation”.

Author's contributions

F.S. and I.F. were responsible for the study design and its supervision. J.K., K.N., and T.D. were responsible for the development of the device. I.F., K.Z., V.K. and J.K. collected the data. D.T. and E.B. were responsible for data preprocessing and analysis. R.Z. and B.B. contributed to the study conception and design. F.S. wrote the original manuscript draft. All authors read and edited the final manuscript.

Acknowledgements

Not applicable.

References

1. Ferrari F, Shell CE, Thumser ZC, Clemente F, Plow EB, Cipriani C, et al. Proprioceptive augmentation with illusory kinaesthetic sensation in stroke patients improves movement quality in an active upper limb reach-and-point task. Front Neurorobot. 2021 Mar 1;15:610673.
2. Goodwin GM, McCloskey DI, Matthews PB. The contribution of muscle afferents to kinaesthesia shown by vibration induced illusions of movement and by the effects of paralysing joint afferents. Brain. 1972 Jan 1;95(4):705–48.
3. Naito E, Roland PE, Ehrsson HH. I feel my hand moving. Neuron. 2002 Dec 5;36(5):979–88.
4. Naito E, Ehrsson HH, Geyer S, Zilles K, Roland PE. Illusory arm movements activate cortical motor areas: a positron emission tomography study. J Neurosci. 1999 Jul 15;19(14):6134–44.
5. Radovanovic S, Korotkov A, Ljubisavljevic M, Lyskov E, Thunberg J, Kataeva G, et al. Comparison of brain activity during different types of proprioceptive inputs: a positron emission tomography study. Exp Brain Res. 2002 Apr 5;143(3):276–85.
6. Naito E, Ehrsson HH. Kinesthetic illusion of wrist movement activates motor-related areas. Neuroreport. 2001 Dec 4;12(17):3805–9.
7. Landelle C, Anton JL, Nazarian B, Sein J, Gharbi A, Felician O, et al. Functional brain changes in the elderly for the perception of hand movements: A greater impairment occurs in proprioception than touch. Neuroimage. 2020 Oct 15;220(117056):117056.
8. Kavounoudias A, Roll JP, Anton JL, Nazarian B, Roth M, Roll R. Proprio-tactile integration for kinesthetic perception: an fMRI study. Neuropsychologia. 2008 Jan 31;46(2):567–75.
9. Naito E, Nakashima T, Kito T, Aramaki Y, Okada T, Sadato N. Human limb-specific and non-limb-specific brain representations during kinesthetic illusory movements of the upper and lower extremities: Human kinesthesia for the four extremities. Eur J Neurosci. 2007 Jun 1;25(11):3476–87.
10. Cignetti F, Vaugoyeau M, Nazarian B, Roth M, Anton JL, Assaiante C. Boosted activation of right inferior frontoparietal network: a basis for illusory movement awareness. Hum Brain Mapp. 2014 Oct 5;35(10):5166–78.
11. Schneider C, Marquis R, Jöhr J, Lopes da Silva M, Ryvlin P, Serino A, et al. Disentangling the percepts of illusory movement and sensory stimulation during tendon vibration in the EEG. Neuroimage. 2021 Nov 1;241(118431):118431.
12. Kodama T, Nakano H, Katayama O, Murata S. The association between brain activity and motor imagery during motor illusion induction by vibratory stimulation. Restor Neurol Neurosci. 2017 Nov 21;35(6):683–92.
13. Hagura N, Takei T, Hirose S, Aramaki Y, Matsumura M, Sadato N, et al. Activity in the posterior parietal cortex mediates visual dominance over kinesthesia. J Neurosci. 2007 Jun 27;27(26):7047–53.
14. Hagura N, Oouchida Y, Aramaki Y, Okada T, Matsumura M, Sadato N, et al. Visuokinesthetic perception of hand movement is mediated by cerebro-cerebellar interaction between the left cerebellum and right parietal cortex. Cereb Cortex. 2009 Jan;19(1):176–86.
15. Bisio A, Biggio M, Avanzino L, Ruggeri P, Bove M. Kinaesthetic illusion shapes the cortical plasticity evoked by action observation. J Physiol. 2019 Jun 1;597(12):3233–45.
16. Bates D, Mächler M, Bolker B, Walker S. Fitting linear mixed-effects models Usinglme4. J Stat Softw. 2015 Oct 7;67(1):1–48.
17. Kuznetsova A, Brockhoff PB, Christensen RHB. LmerTest package: Tests in linear mixed effects models. J Stat Softw. 2017 Dec 6;82(13):1–26.
18. Hanakawa T, Dimyan MA, Hallett M. Motor planning, imagery, and execution in the distributed motor network: a time-course study with functional MRI. Cereb Cortex. 2008 Dec 20;18(12):2775–88.
19. Jeannerod M. Neural simulation of action: a unifying mechanism for motor cognition. Neuroimage. 2001 Jul 1;14(1 Pt 2):S103–9.
20. Lotze M, Halsband U. Motor imagery. J Physiol Paris. 2006 Jun 1;99(4-6):386–95.
21. Bolognini N, Maravita A. Proprioceptive alignment of visual and somatosensory maps in the posterior parietal cortex. Curr Biol. 2007 Nov 6;17(21):1890–5.
22. Craig ADB. How do you feel--now? The anterior insula and human awareness. Nat Rev Neurosci. 2009 Jan;10(1):59–70.
23. Alexander GE, DeLong MR, Strick PL. Parallel organization of functionally segregated circuits linking basal ganglia and cortex. Annu Rev Neurosci. 1986 Mar 1;9(1):357–81.
24. Lehéricy S, Benali H, Van de Moortele PF, Pélégrini-Issac M, Waechter T, Ugurbil K, et al. Distinct basal ganglia territories are engaged in early and advanced motor sequence learning. Proc Natl Acad Sci U S A. 2005 Aug 30;102(35):12566–71.
25. Grillner S, Robertson B, Kotaleski JH. Basal ganglia-A motion perspective. Compr Physiol. 2020 Sep 24;10(4):1241–75.
26. Dan B. Neuroscience underlying rehabilitation: what is neuroplasticity? Dev Med Child Neurol. 2019 Nov 1;61(11):1240.

Figures

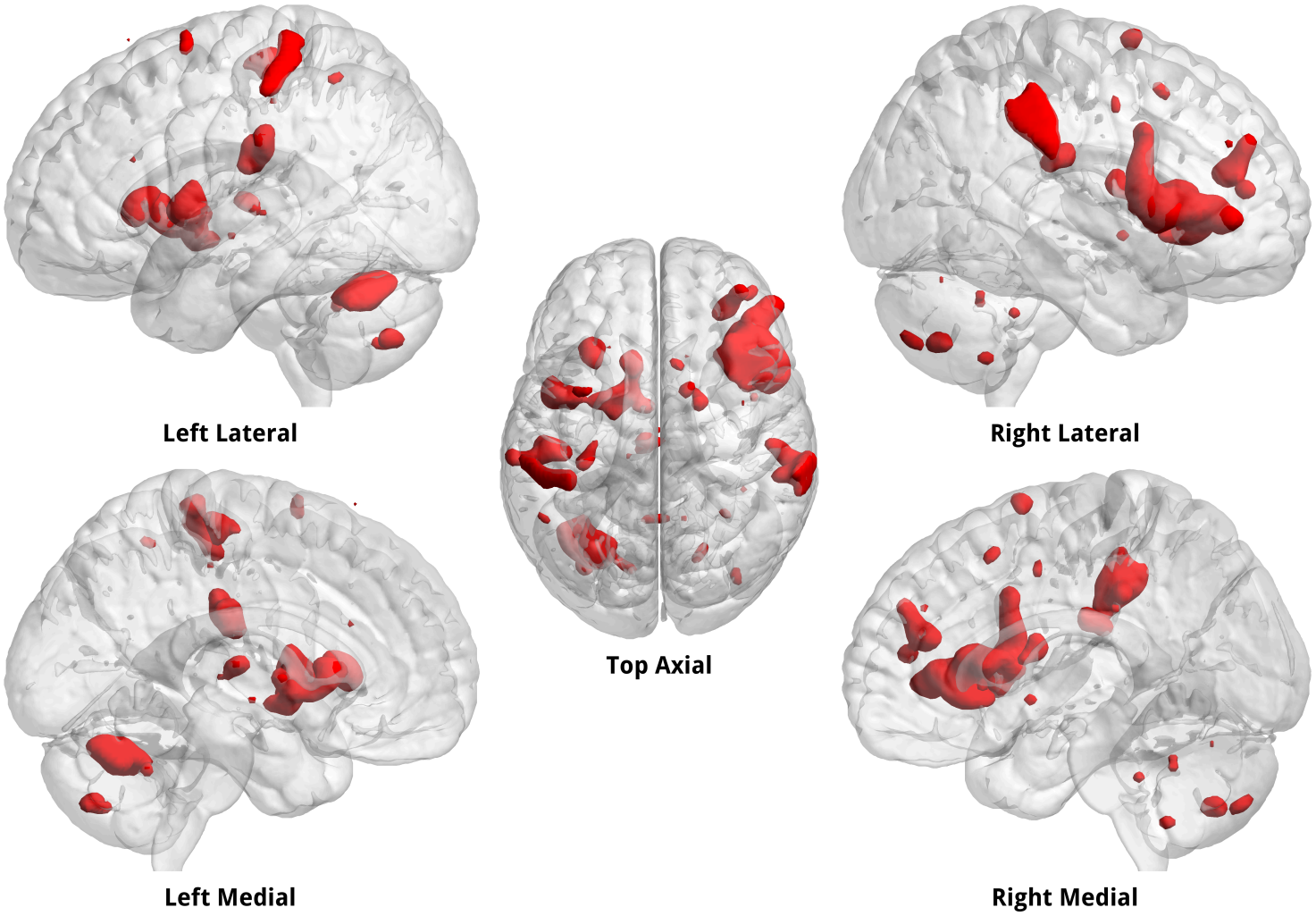


Figure 1

Group-level analysis comparing the vibration-induced kinesthetic illusion to the control condition. Results are thresholded at T = 3.93 ($p < 0.001$, uncorrected for multiple comparisons).

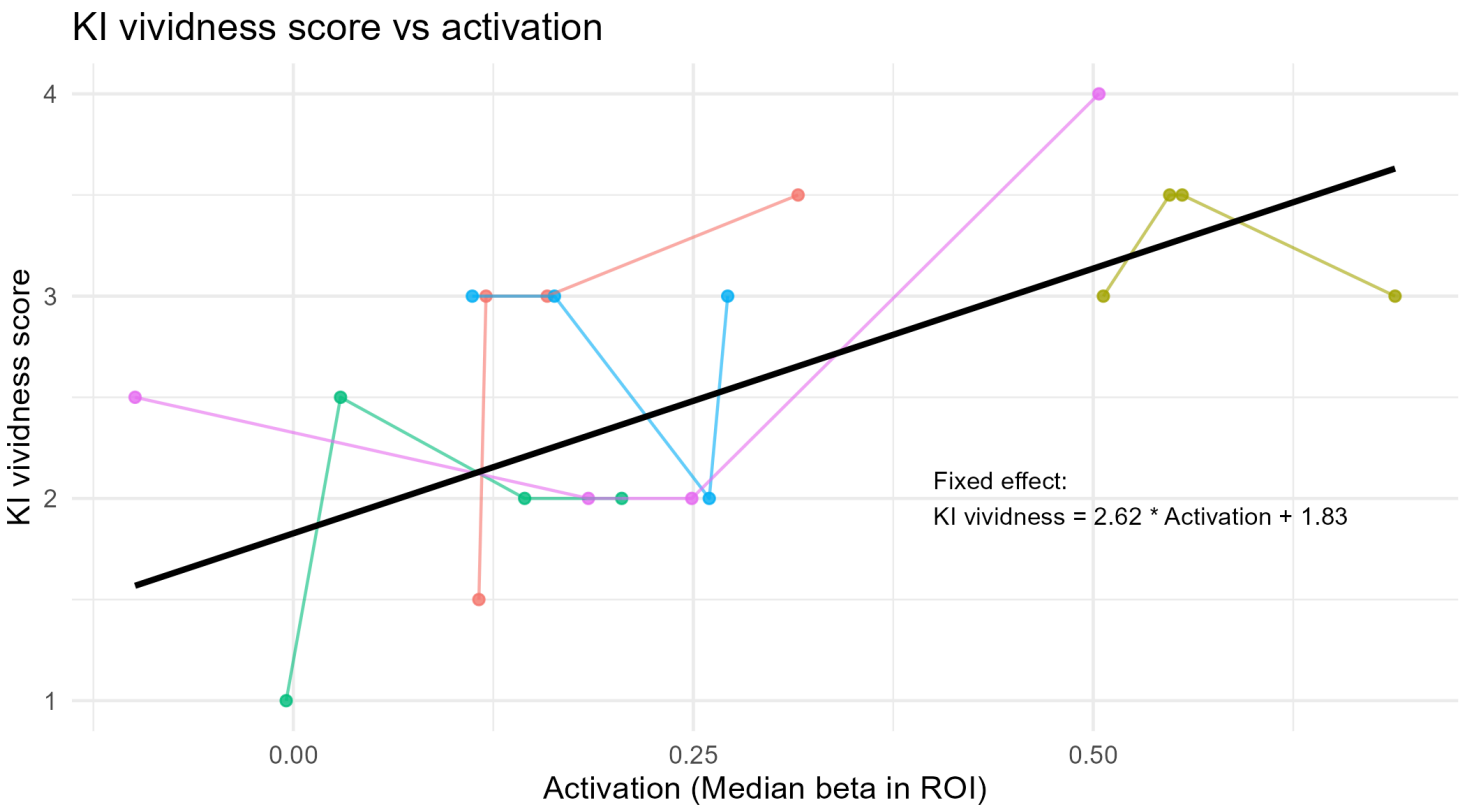


Figure 2

Reported kinesthetic-illusion rating score and the cortical activation (median beta coefficient within the ROI, depicted in Fig.1). The trend line illustrates the fixed-effect part of the resulting mixed-effect model. Individual participants are color-coded.

Supplementary Files

This is a list of supplementary files associated with this preprint. Click to download.

- SuplementaryMaterials.docx